C. R. Physique 3 (2002) 509–521

Électromagnétisme, optique/*Electromagnetism, optics*
(Atomes, molécules/*Atoms, molecules*)

DOSSIER

PHOTONIQUE MOLECULAIRE : MATÉRIAUX, PHYSIQUE ET COMPOSANTS

MOLECULAR PHOTONICS: MATERIALS, PHYSICS AND DEVICES

Universality in unintentional laser resonators in π-conjugated polymer films

Randall C. Polson *, **Mikhail E. Raikh, Z. Valy Vardeny**

Department of Physics, University of Utah, Salt Lake City, UT 84112, USA

Accepted 1 March 2002

Note presented by Guy Laval.

Abstract When films of π-conjugated polymers are optically excited above a certain threshold intensity, then the emission spectrum acquires a multimode finely structured shape, which depends on the position of the excitation spot. We demonstrate that the power Fourier transform (PFT) of the emission spectrum exhibits a certain peak-like structure, which also depends on the excitation spot. Our intriguing observation is that *averaging* the individual PFTs does not lead to a *structureless* curve, but rather yields a series of *distinct* transform peaks. This suggests *universality*, namely that the underlying random resonators that are responsible for the laser emission from the π-conjugated polymer film are almost *identical*. We argue that the reason for such an universality is the large size of a typical resonator, which we determined from the PFT, as compared to the emission wavelength, λ. This fact is, in turn, a consequence of the large light mean free path, $l^* \simeq 10\lambda$ in the polymer film. This contrasts previous observations of random lasing in powders, where $l^* \sim \lambda$. We develop a simple theory that explains the presence of peaks in the average PFT and predicts their shape. The results of the theory agree *quantitatively* with the data. ***To cite this article: R.C. Polson et al., C. R. Physique 3 (2002) 509–521.*** © 2002 Académie des sciences/Éditions scientifiques et médicales Elsevier SAS

random lasing / Fourier transform / π-conjugated polymer

1. Introduction

Random lasing is a young and rapidly growing area of research. In fact, the phenomena 'random lasing' comprise two distinctively different subfields of thorough theoretical and experimental studies. We dub them here 'incoherent' random lasing and 'coherent' random lasing, respectively. The essence of both subfields is the propagation of light in random media with gain.

Incoherent random lasing corresponds to a situation where, in the absence of a resonator, multiple scattering prevents light from leaving the optically pumped region. Such a disorder-induced feedback is sufficient for a drastic narrowing of the emission spectrum above a certain threshold pump intensity. Research on incoherent random lasing addresses various aspects such as steady state spectral characteristics

* Correspondence and reprints.
E-mail address: rpolson@physics.utah.edu (R.C. Polson).

S1631-0705(02)01336-1/FLA

and dynamics of this narrowing. *Coherent random lasing*, on the contrary pursues a scenario where disorder in a random medium leads to complete (or nearly complete) localization of the photonic modes. In other words, the disorder assumes the role of a Fabry–Perot resonator in a conventional laser. Therefore, above a threshold excitation intensity the emission spectrum from such a disordered medium comprises of a number of very sharp, laser-like lines.

The message of the present paper is that within the subfield of coherent random lasing there exist two different regimes, which we dub here 'quantum' and 'classical'. These two regimes are analogous to the quantum (Anderson) and classical localization of electrons in a random potential. If the potential is short-range, then the only length scale associated with it is the elastic mean free path, l^*. Increasing disorder decreases the value of l^*. Anderson localization is expected when l^* becomes smaller than λ, where λ is the electronic wavelength. In contrast to the short-range potential, the long-range potential can be envisioned as a smooth landscape consisting of 'lakes' and 'mountains'. If a typical spatial scale of this potential is much bigger than λ, then it is obvious that electrons with energies near the bottom of each lake are localized. The origin of this localization is purely classical. Interference effects, which are crucial for Anderson localization play a secondary role in the classical localization scenario; they are responsible only for the *exact* positions of the energy levels inside the lakes. Within this picture, the localization length of the electronic states is of the order of the lake diameter, and thus much bigger than λ.

Since there is no one-to-one correspondence between the Schrödinger equation and the wave equation, the above picture of the classical localization cannot be directly applied to light. Nevertheless, as we argue below, the long-range fluctuations of the refraction index, $n(\boldsymbol{\rho})$ are able to trap the light. The analog of a lake in optics is a region with higher $n(\boldsymbol{\rho})$ than the average n of the surrounding space. Classical localization is then due to the total internal reflections from the boundaries of this region, as follows from geometrical optics.

In this paper we present evidence that coherent random lasing from π-conjugated polymer films is of the *classical type*. The basic argument in favor of this conclusion is that a long-range fluctuation of $n(\boldsymbol{\rho})$ is similar to a Fabry–Perot resonator, in the sense that it gives rise to a *number* of localized modes having close frequencies and close quality factors. These modes are revealed in the emission spectrum. Since the frequencies of such modes are correlated, we could estimate the size, L of the underlying resonators from the power Fourier transform (PFT) of the spectrum. We indeed find that $L \gg \lambda$.

The most probable reason for the fluctuations of $n(\boldsymbol{\rho})$ in the polymer films is inhomogeneity of the film thickness, h. Since light is confined within the film due to waveguiding (see Fig. 1(a)), larger h leads to higher in-plane wave vector of the light modes, i.e. to higher *effective* refraction index. By virtue of this mechanism, the long-range fluctuation of h can result in the formation of a microdisk-type resonator (Fig. 1(b)). Such resonators have recently attracted a lot of attention [1,2], since they constitute the key element of semiconductor microlasers.

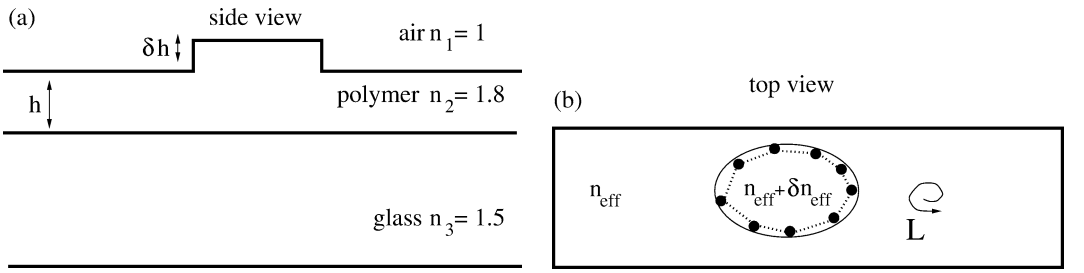

Figure 1. (a) Schematic illustration of the thickness fluctuation of the polymer film; the refractive indices of the polymer and glass substrate are given. (b) Schematic illustration of the whispering-gallery type mode in a resonator formed by a thickness variation δh; L is the round trip resonator path-length.

Certainly, alongside with long-range $n(\boldsymbol{\rho})$ fluctuations, short-range disorder is also present in the polymer films. This leads to $l^* \simeq 10\lambda$, which we determined from coherent backscattering measurements. Such a weak short-range disorder is unable to localize light by itself. However, it radically affects lasing from the polymer film. This is because, whereas $l^* \gg \lambda$, it is still much shorter than the resonator size, i.e. $l^* \ll L$; this means that the ability of most random resonators to trap light is suppressed by the short-range disorder. There is a dramatic consequence of such a suppression: those resonators that 'survive' the short-range disorder are sparse, and consequently *almost identical*. This scenario manifests itself in a spectacular way. At each position of the excitation spot the PFT of the random emission spectrum exhibits certain features. We found that averaging the PFTs of individual random spectra over the positions of the excitation spot on the polymer film not only does not smear these features, but, on the contrary, yields a series of *distinct* transform peaks. Moreover, we found that the shape of the averaged PFT is *universal*, i.e. increasing the disorder and correspondingly reducing l^* does not change this shape; the average of the PFT spectra at different l^* scales with l^* to a universal curve. We have also developed a simple theory for the the PFT. Without specifying the shape of the resonators, the theory is based on a *single* assumption that the random resonators are *exponentially* sparse. This assumption is sufficient to reproduce the universal shape of the average PFT.

The paper is organized as follows. In Section 2 we review the current state of the theory and the experiment in the subfields of coherent and incoherent random lasing. In Section 3 we report on our measurements of random lasing spectra, PFTs and spatial intensity distribution of the emission from $DOO-PPV$ polymer films. In Section 4 a simple theory of random resonators formed due to long-range fluctuations of $n(\boldsymbol{\rho})$ is presented. Section 5 concludes the paper.

2. Review of random lasing

2.1. Incoherent random lasing: theory

The first theoretical analysis of random lasing dates back to 1967 [3]. In the seminal paper of Letokhov [3] a random laser was modeled by an homogeneously pumped medium with scatterers that is contained within a certain volume. Due to the excitation pump, light diffusion inside the medium is accompanied by optical amplification. Lasing threshold is then determined from the condition that, in course of diffusion through the volume, light is amplified by a factor of ~ 2. Such an amplification compensates for the losses from the surface. The key idea of the theory [3] is that multiple scattering leads to *incoherent feedback* by forcing the light to spend a relatively long time inside the amplification region. Since light amplification can be viewed as multiplication of the number of photons, the condition for lasing is analogous to the criticality condition for chain reaction.

Interest revival in diffusive propagation of light in disordered gain media [4] has triggered further advancement of the incoherent random lasing theory. In the original work [3] it was assumed that the optical active centers are located inside the *same* particles that scatter light. The immediate consequence of this assumption is that a critical gain is independent of the scatterers concentration. To model realistic systems, the common situation that was considered in later papers was a homogeneous laser dye solution with suspended passive scattering microparticles. In this case, the description of random lasing requires solving the system of coupled equations for light diffusion with amplification, and also for population inversion. Various versions of such a system were invoked [5–9] to study the steady state [5,9] as well as the dynamical [6–8] properties of laser action in the scattering gain media.

In [5] a generic model of a dye with singlet and triplet electronic excitations was considered. Taking into account the possibility that the emitted light from the singlet band can serve as a pump for the triplet band yielded a bichromatic emission above a certain excitation threshold with a ratio of emission peaks depending on the pump intensity and dye concentration. In [6–8] the temporal response of a disordered laser material to the incident pump (or pump and probe [6]) pulses was studied using a Monte Carlo simulation of random walk of the pump and emitted photons, which are interrelated through the population rate equation.

These studies revealed a rich emission dynamics at excitation intensity close to the threshold. Finally, in [9] the Monte Carlo simulation was employed to study the emission spectral narrowing above the excitation threshold, as well as the input-output dependencies.

Summarizing, the original model of [3] yields a transparent and very appealing *quantitative* description of the incoherent random lasing process. However it leaves out two important physical effects: namely interference of diffusively moving waves, which is a precursor of photon localization [10–16] and strong interference-induced fluctuations of the local light intensity, i.e. the mesoscopic phenomena [17–19]. The fundamental role of the two effects was not appreciated back in 1967.

2.2. Incoherent random lasing: experiment

The experimental results reported in the literature [20–40] essentially confirm the theoretical predictions. Except for studies on powder grains of laser crystal materials [36–38] and π-conjugated polymer films [39, 40], the majority of experiments [20–35] have used dye solutions as amplifying media. Colloidal particles suspended in a solution served as random scatterers. In a typical experiment a short pulse is used for excitation. For below threshold pump intensities the emitted pulse is long. It shortens drastically to $\lesssim 50$ ps as the laser threshold is exceeded. The emission spectrum narrows to $\lesssim 20$ nm. Numerical solution of the the radiative transfer equations [3,5–9] yield the understanding of the dependence of the threshold energy on the concentration of scatterers, concentration of dye, cavity size, etc. However, the most convincing proof that laser action is due to 'diffusive feedback' stems from the fact that below threshold the presence of scatterers has practically no effect on the emission.

2.3. Coherent random lasing: theory

During the last decade the interplay of interference-induced localization effects and amplification of light in random media was the subject of intensive theoretical [41–49] studies. The theoretical prediction [41] that longer diffusive trajectories due to gain result in sharpening of coherent backscattering cone has been confirmed experimentally [14].

The next step was incorporation of disorder and interference into the conventional system of Maxwell equations coupled with the rate equations for the electronic population of a four-level system involved in lasing. This program was realized in [50] for a model system representing a sequence of one-dimensional layers of random thickness. One-dimensional nature of the model and large (four times) contrast in dielectric functions between the neighboring layers allowed the authors to trace the crossover between the weak disorder i.e. long localization length (compared to the system size) and strong disorder regimes. The simulations of [50] have confirmed the basic idea of random lasing that increasing the disorder results in decreasing of the lasing threshold. These simulations have also verified that lasing lines in the emission spectrum have their origin in the localized modes of the disordered one-dimensional system. Further studies reported in [51] have indicated that the distribution of electromagnetic field in the lasing mode is practically the same as in the localized mode in the absence of gain. The dependence of the emission spectrum on the gain frequency was also studied in the simulations of [51]. It was demonstrated that, upon varying the gain frequency, the order in which different localized modes overcome the lasing threshold can change.

2.4. Coherent random lasing: experiment

Recently a group of experiments was reported [52–55], which revealed features of random lasing *qualitatively* different from those reported previously in [20–35].

The disordered gain media in which these measurements were done were very different, ranging from ZnO polycrystalline powders [52,53] to π-conjugated polymer films [54], organic dyes-doped gel films [54] and dye-infiltrated opal photonic crystals [55]. However, a unifying feature of the results reported using these media was the evolution of the emission spectra with increasing excitation intensity. Namely, the broad photoluminensce band at low intensities first drastically narrows; as the excitation intensity was

increased even further, the emission spectrum transforms into a fine structure that consists of a number of sharp ($\delta\lambda < 1$ nm) laser-like emission lines. Using the photon counting statistics [56], the coherent nature of the emitted light has been proved for powders [57] as well as for polymer films [58].

The most comprehensive experimental study of random lasing thus far has been performed by Cao et al. [52,53] on ZnO powders that are extremely efficient scattering media [59]; the light mean free path, l^* extracted from coherent backscattering measurements was $l^* = 0.8\lambda$ in [52] and $l^* = 0.5\lambda$ in [53]. On the basis of measurement of spatial distribution of the emitted light complemented with numerical simulations [53] it was demonstrated that the underlying mechanism of lasing was formation of closed loop paths of light with a characteristic size comparable to λ. These paths are formed due to multiple scattering. It was argued in [52] that, due to interference or, in other words, localization effects, such closed loop paths serve as resonant cavities for light. Thus, the formation of these tiny cavities provides the feedback necessary for lasing. Correspondingly, the positions of the emission lines are determined by particular configurations of scatterers constituting each cavity [53].

The evolution of the emission spectrum with pump power observed in [52] is in qualitative agreement with numerical results of [50] obtained for the domain of small localization lengths.

3. Experimental results

3.1. Preliminary discussion

In this paper we demonstrate that despite the similarity in the evolution of the emission spectra, the mechanism of random lasing in π-conjugated polymer films is fundamentally different from that reported for powders in [52,53]. The difference can be briefly formulated as follows: In the case of [52,53] it was reported that *one* emission line per random cavity was detected, whereas in polymer films one resonator gives rise to a *number* of correlated emission lines. This is because in our experiments with polymer films the relevant random resonators are much bigger in size; this is not surprising since the mean free path l^* in the polymer film was measured to be $l^* \sim 10\lambda$. Our principal finding is that all random resonators are approximately *identical*. We come to this conclusion on the basis of the *regularity* in the experimentally observed emission spectra. Similarly to the case of electron transport in which the underlying period has been experimentally discerned from magnetoresitance *fluctuations* [60], the regularity in the *random* emission spectra is revealed here upon Fourier analysis of the data.

3.2. Designed resonance structures

The main tool that will be employed in the investigation of random lasing is the Fourier transform of the emission spectra. To gain some insight and intuition, this analysis will be performed with carefully constructed resonance cavities. The first structure will be a microring and the second structure will be a microdisk. Both structures support whispering gallery modes and rely on total internal reflection to confine light.

A microring laser is fabricated by forming a thin coating of the gain medium polymer on a glass core. This structure is easily fabricated and has a high quality factor, Q. The conjugated polymer poly(dioctyloxy) phenylene vinylene (DOO-PPV), which was synthesized by modifying a published procedure [61], is an example of a medium to form this structure. Figure 2(a) is an emission spectra of a microring with a core diameter of 125 μm and a coating with is roughly 1 micron thick. The microring was optically excited using 100 ps pulses from the second harmonic of a Nd : YAG regenerative amplifier that operated at 100 Hz repetition rate.

The emission spectrum of the microring has many narrow emission lines. The spacing of the peaks fits that of a Fabry–Perot resonator where the roundtrip length, $2nL$, is replaced the by circumference, $\Delta\lambda = \lambda^2/2nL = \lambda^2/n\pi D$ where n is the index of refraction and D is the diameter. The peak spacing in Fig. 2(a) is 0.7 nm, which corresponds to an index of refraction of $n = 1.46$. This is an intermediate value

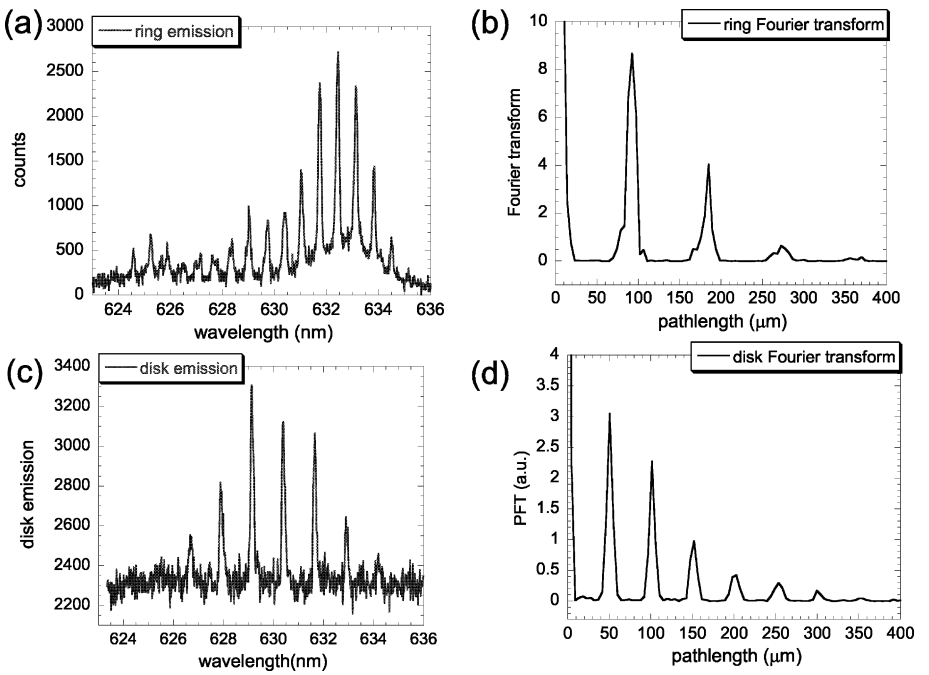

Figure 2. (a) The emission spectrum of a DOO-PPV microring laser. (b) Fourier transform of the spectrum in (a). (c) The emission spectrum of a DOO-PPV microdisk laser. (d) Fourier transform of the spectrum (c).

between the glass core $n = 1.44$ and the polymer $n = 1.8$, which indicates that the field penatrates into the glass core.

Fig. 2(b) is the Fourier transform of Fig. 2(a). There is a series of equally spaced diminishing peaks. By measuing the spectrum in wavevector ($k = 2\pi/\lambda$) the units of the Fourier transform come out in length. The expected Fourier transform of a Fabry–Perot cavity has peaks occuring at $b = nL/\pi$ [66,67]. For the circular geometry used here the round trip length is replaced by the circumference and the Fourier transform has peaks at $nD/2$.

In the transform space peaks occur every 82 μm. Assuming a diameter of 125 μm the index of refraction is 1.47, which is an intermediate value between the polymer and supporting glass, and agrees with the value for a Fabry–Perot cavity. This value from the Fourier transform for nD is more accurate than the value from the emission line spacing and can be used to assign each emission line to a Bessel function [68].

The second known resonator is a microdisk. These structures are formed with photolithography where the final structure is a disk on a glass substrate. Typical dimensions are 55 μm diamter and 1 μm thickness. Fig. 2(c) is the emission spectrum of an optically excited microdisk. Again many narrow emission peaks are observed. The Fourier transform, Fig. 2(d), shows equally spaced peaks spaced at 51 μm. With a diameter of 55 μm, this gives an index of refaction of $n = 1.83$ indicating that the fields are completely confined in the disk.

3.3. Random spectra and Fourier transforms

We will now focus on a polymer film. Fig. 3(a) is a typical emission spectrum above the laser threshold which was measured from a film excited with a stripe illumination of 2 mm $\times 100$ μm that is formed using a cylindrical lens. We note that in contrast, the excitation spot in [52,53] was much smaller in size ~ 20 μm. Note also, that, despite the fact that in our case the two sizes of the excitation stripes differ by a factor of twenty. Nevertheless they both are *much bigger* than l^*. Clearly therefore, the excited area

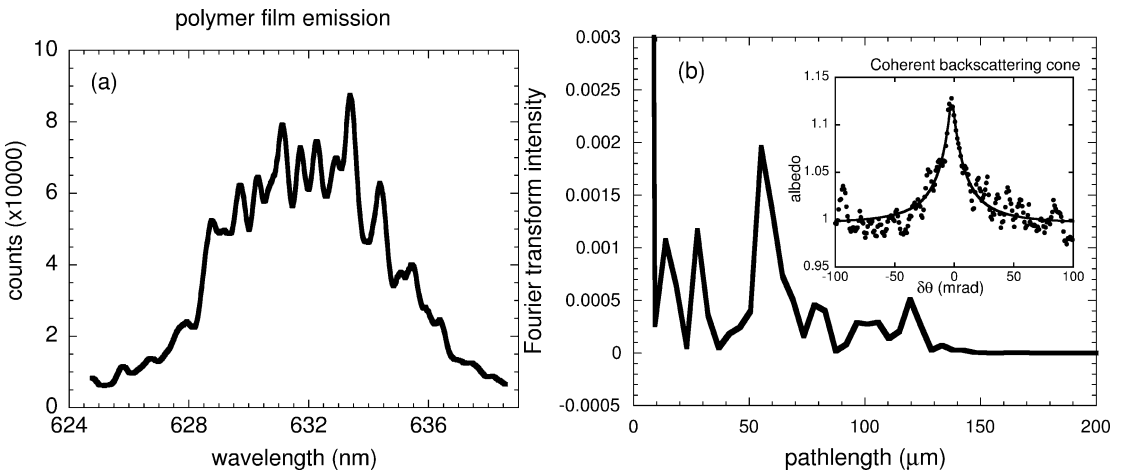

Figure 3. (a) The measured emission spectrum of a DOO-PPV film above the threshold intensity for lasing. (b) Power Fourier transform of the emission spectrum in (a). The inset shows the coherent backscattering cone from a bulk sample of DOO-PPV.

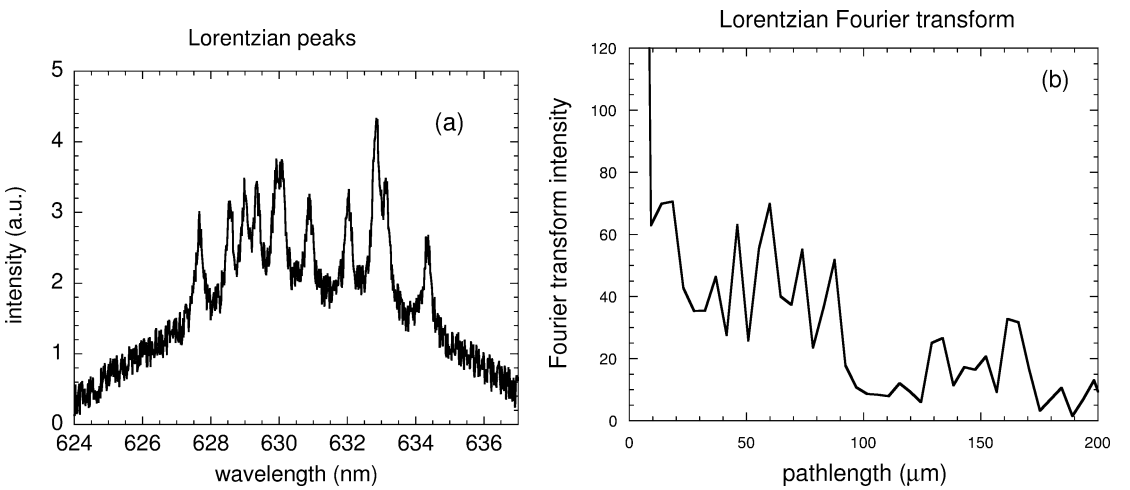

Figure 4. (a) A generated emission spectrum that consists of 12 Lorentzians. (b) Power Fourier transform of (a).

cannot be considered as one dimensional [50,51]. The spectrum was measured at an excitation intensity of 0.2 μj/(pulse·mm) using 100 ps pulses from the second harmonic of a Nd : YAG regenerative amplifier that operated at 100 Hz repetition rate. The specific polymer again was poly(dioctyloxy) phenylene vinylene.

Fig. 3(b) shows the PFT of Fig. 3(a) and contains many apparent features. In general, the presence of such features in the PFT does not prove regularity in the emission spectrum. To illustrate this, we have generated a spectrum very similar to Fig. 3(a) by adding 12 Lorentzians centered at random wave lengths with random linewidths. Fig. 4(a) is a numerically simulated spectrum and Fig. 4(b) is the corresponding PFT, which also shows many apparent features. Next we generated 125 random spectra similar to Fig. 4(a), and averaged their individual PFTs. As would be expected, the sharp PFT features vanished upon averaging. However when a similar procedure was performed on 125 *real* laser emission spectra obtained by shifting the excitation stripe on the surface of the polymer film, some features *persisted* in PFT; moreover, they

became much more pronounced, as seen in Fig. 6 solid line. This supports the above statement about universality made in the Introduction.

Similarly to the features in magnetoresitance, which serve as fingerprints of actual disorder realization [60], the peaks in a single PFT reveal the properties of an individual random resonator. In Fig. 3(b) the peaks allow us to determine the size of a lasing resonator; more precisely the length L of the light path is calculated via the relation $L = \pi d/n$, where d is the peak position in the PFT and n is the polymer index of refraction. Using $n = 1.8$ for the DOO-PPV polymer we get from Fig. 3(b) a round trip length $L = 56$ μm for the peak at $d = 18$ μm, and $L = 216$ μm for the peak at $d = 60$ μm, respectively. The smaller cavity corresponds to a length $L = 90\lambda$, which greatly exceeds the length scale $\sim \lambda$ as observed in [52,53]. It is also important to note that the length L also largely exceeds the light mean free path, l^*, which was determined in DOO-PPV sample to be $l^* = 5.2$ μm or 8.3λ from the width of the coherent backscattering cone [62] as shown in Fig. 3(b), inset.

3.4. Spatial intensity distribution

Fig. 5 is a magnified image of approximately half of the excited area on the polymer film and measures the spatial distribution of the emission intensity at an excitation intensity above the laser threshold. The magnification is approximately 60 times. The emission intensity was measured through a long pass filter to remove the pump excitation light and avoid saturating the image array. The z-axis was computed by scaling the emission intensity of the red component of the color image. A crude estimate of the distance between the bright emitting spots is 40 μm, which is roughly comparable to that measured in [53]. However there is a stark difference between Fig. 5 here and the corresponding spatial distribution in [53], namely that in our

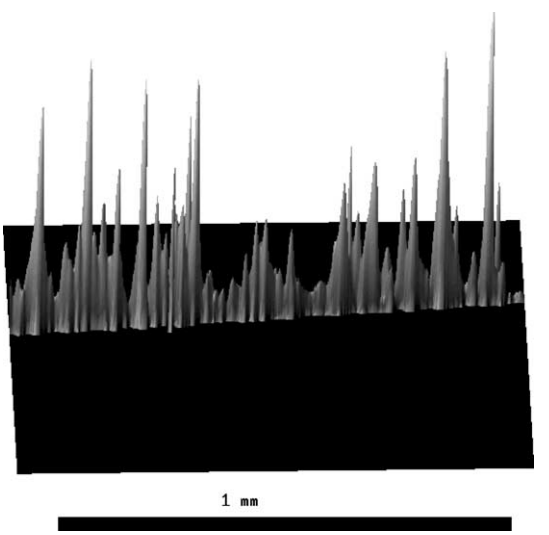

Figure 5. The measured spatial distribution of the emission intensity in the DOO-PPV film under condition of random lasing.

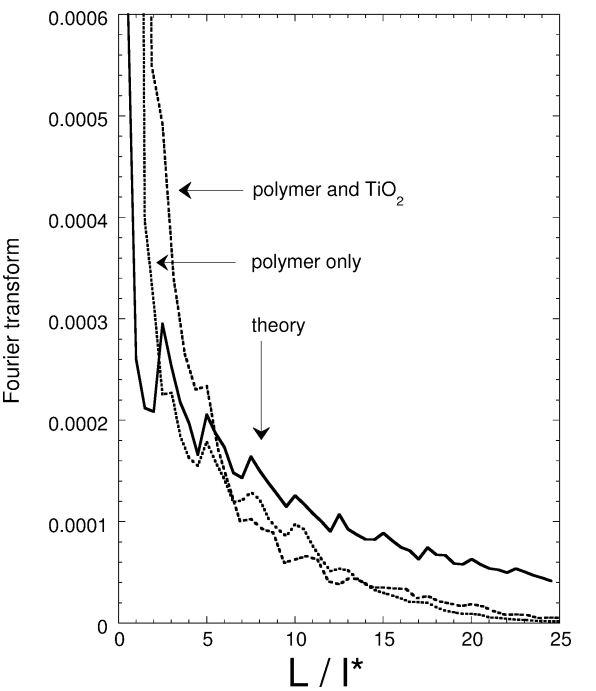

Figure 6. Average of 125 power Fourier transforms scaled by l^*. The solid line is a theoretical model based on Eq. (5) superimposed on a smooth background; dotted lines are emission of pure polymer, and polymer doped with TiO_2 scatterers, respectfully.

case there are *many more* bright spots than spectral lines in the emission spectrum, as shown in Fig. 3(a). On the other hand, bright spots *must* correspond to certain lines in the emission spectrum. Recall, that from the PFT a characteristic size of the resonator $L = 56$ μm was inferred above. In the scale of Fig. 5 this corresponds to a single bright spot. The total number of bright spots in Fig. 5 is approximately three times the number of emission lines in Fig. 2(a). Thus, the emission spectrum which contains a limited number of lines reflects the emission from *many* resonators. The only resolution to this seemingly paradoxical situation is that all the resonators that are responsible for lasing in the polymer film are *approximately the same*. This fact, and the shape of the averaged PFT spectra seen in Fig. 6 require a theoretical explanation, which is given below.

4. Theory

We do not really know the actual shape of the random resonators in the polymer films. However, it is apparent that our case is very different from the case in [52,53] since the round trip length, L of a typical resonator is much bigger than the mean free path l^*, which, in turn, is much bigger than the wavelength λ.

Large values of L suggest that the resonators are formed due to the long-range inhomogeneities of the refraction index, $n(\boldsymbol{\rho})$. A plausible microscopic origin of these inhomogeneities is the fluctuation δh of the polymer film thickness, h, as illustrated in Fig. 1(a). Due to the waveguiding in the polymer film, the effective refraction index, n_{eff}, describing the in-plane propagation of light, is related to n as

$$n_{\text{eff}} = \sqrt{n^2 - (p+1)^2\left(\frac{\lambda}{2h}\right)^2},$$

where p is the number of the transverse waveguide mode. Therefore, a local increase of the film thickness by δh ($\ll h$) results in the enhancement of n_{eff} (see Fig. 1(a)) by $\delta n_{\text{eff}} = (p+1)^2\lambda^2\delta h/4nh^3$.

In fact, long-range variations of the film thickness in DOO-PPV polymer films were reported in [63]. Since $\delta h \ll h$, and thus $\delta n_{\text{eff}} \ll n_{\text{eff}}$, the angle of total internal reflection from the boundary (Fig. 1(b)) is close to 90°.

Thus, the microdisk-type resonator that is formed due to fluctuations of the film thickness (Fig. 1(b)) can only support the 'whispering-gallery', but not the 'bow-tie' modes [2].

Below we demonstrate that the only assumption necessary to predict the shape of the average PFT is that the formation of resonators with $L \gg l^*$ is highly unlikely. In other words, we assume that the the areal *density*, $g(L)$, of resonators with a given length L falls off exponentially with L. Quantitavely this fact can be expressed as follows:

$$g(L) = \frac{1}{l^{*2}}\exp\bigl(-\varphi(L)\bigr), \tag{1}$$

where the function $\varphi(L)$ increases with L, so that for $L \gg l^*$ we have $\varphi(L) \gg 1$. The actual form of the function $\varphi(L)$ is determined by the type of disorder in the film. For a given area of the excitation spot, S, the maximal size, L_S of the resonator *present* within the area is determined by the condition $Sg(L_S) \sim 1$ [64]. Since $g(L)$ is exponentially steep, this condition defines L_S with high accuracy. For values of L close to L_S, i.e. $|L - L_S| \ll L_S$, we can expand $\varphi(L)$ as follows:

$$\varphi(L) = \varphi(L_S) + \frac{L - L_S}{l_0}, \tag{2}$$

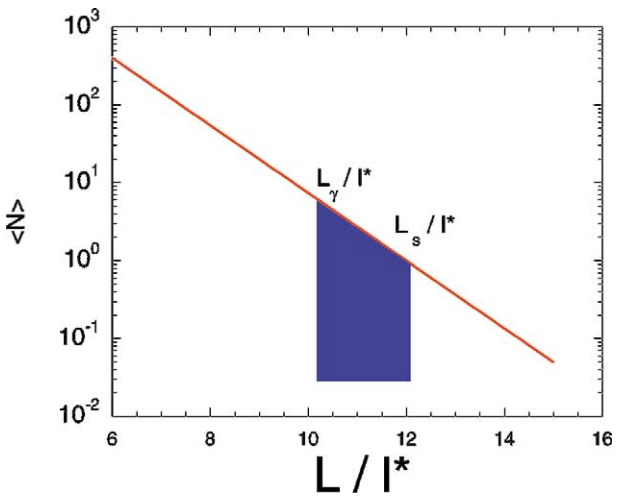

Figure 7. The average number of resonators $\langle N \rangle$ that exist within a sample with area S plotted versus the dimensionless pathlength L/l^* (Eq. (3)). L_γ is the minimum length that is required to overcome losses. The shaded area represents resonators that are able to lase.

where $l_0^{-1} = (\partial\varphi/\partial L)_{L=L_S}$. Using Eq. (2) the average number N of resonators with the path length L within the illuminated area can be presented as

$$\langle N(L) \rangle = \exp\left(\frac{L_S - L}{l_0}\right). \tag{3}$$

The function $\langle N(L) \rangle$ is shown in Fig. 7. At this point we note that for a given gain, γ, there is a *minimum* resonator length, L_γ, which is required to ensure lasing. For example, in the realization of a random resonator shown in Fig. 1 this length is determined by the condition $\exp(\gamma L)F(L/L_c) = 1$, where the function F accounts for losses originating from the 'tunneling escape' of light due to the curvature of the resonator perimeter [65]. The characteristic length L_c is related to the variation δn_{eff} as $L_c = \lambda n_{\text{eff}}^{1/2}(\delta n_{\text{eff}})^{-3/2} \gg \lambda$. The asymptotics of the function F at large values of the argument is $F(z) = \exp(-2z/3)$. In principle, there exists another mechanism of losses originating from generically non-circular shape of the resonator [65]. However, for $\delta n_{\text{eff}} \ll n_{\text{eff}}$ the 'tunneling' mechanism is dominant. The key point of our consideration is that, since the function F is steep, the condition $\exp(\gamma L_\gamma)F(L_\gamma/L_c) = 1$ defines the length, L_γ with *high accuracy*.

For the illuminated stripe area S, lasing threshold is exceeded when the gain is sufficiently high. Quantitatively, this condition can be expressed as $L_\gamma < L_S$. When this condition is met, then the lasing resonators have lengths between L_γ and L_S (shaded area in Fig. 7).

The above arguments allow us to express the shape of the *average* PFT. The PFT for a single resonator with a given length, L, can be presented as

$$I(d) = \sum_m A_m \delta\left(mL - \frac{\pi d}{n}\right), \tag{4}$$

where each m is an harmonics index that represents a round trip in the resonator. For all resonators A_m fall off with m, but as gain starts to better compensate for losses, the harmonics amplitudes fall off more slowly [66,67]. The better gain compensates for losses, the slower is the decay of A_m with m. It is usually approximated as r^m [67], where r is a factor close unity; $(1 - r)$ characterizes the proximity to the lasing threshold. Below laser threshold Eq. (4) is exactly valid; however above laser threshold the expected behavior of A_m may change. We have studied previously [68] the change in the behavior of a single cavity crossing the lasing threshold. The results were that upon passing laser threshold the spacing between the

components of the PFT stays the same, whereas the factors A_m decrease in amplitude. In Eq. (4) we used the fact that the spectrum of the resonator is close to a delta function in the vicinity of the threshold [67]. We note that the analysis of the coefficients A_m was recently suggested as a method to quantify resonator losses below lasing threshold [67]. Using Eq. (4) the average (over excitation spots with area S) PFT takes the form

$$\begin{aligned}\big\langle I(d)\big\rangle &\propto \sum_m A_m \int_{L_\gamma}^{\infty} \mathrm{d}L\, \delta\left(mL - \frac{\pi d}{n}\right)\big\langle N(L)\big\rangle \\ &\propto \sum_m \frac{A_m}{m} \exp\left[-m^{-1}\left(\frac{\pi d}{n l_0}\right)\right]\Theta\left(\frac{\pi d}{n} - mL_\gamma\right),\end{aligned} \tag{5}$$

where $\Theta(x)$ is the step-function. Eq. (5) indicates that the average PFT contains structures that are dictated by the length L_γ. Therefore, the presence of structures in Fig. 6 has a simple physical interpretation. Namely, that only resonators with L above a certain, *well-defined value* contribute to the laser emission spectrum. It is also seen from Eq. (5) that the dependence of $\langle I(d)\rangle$ scales with l_0.

4.1. Test of universality

The phenomenological parameter l_0 defined by Eq. (2) is the characteristics of particular type of the disorder in the film. Within a simple model that is illustrated in Fig. 1 with long-range fluctuations of the film thickness playing the role of 'mirrors,' this parameter should coincide with the light mean free path, l^*, which is determined by the short-range disorder. Indeed, as follows from Eq. (3), upon increasing the path length by δL, the number of resonators diminishes by a factor

$$\frac{\langle N(L+\delta L)\rangle}{\langle N(L)\rangle} = \exp\left(-\frac{\delta L}{l_0}\right). \tag{6}$$

On the other hand, this reduction results from the fact that the light is scattered away from the mirrors within the segment δL. The probability to *survive* this scattering is equal to $\exp(-\delta L/l^*)$. Comparing this probability with the r.h.s. of Eq. (6), we conclude that $l_0 = l^*$.

In order to test the prediction that the averaged PFT Eq. (5) scales with l^*, we have intentionally introduced TiO_2 particles into the solution prior to the spin-casting process. From the coherent backscattering measurements on bulk samples, we have established that an additional short-range disorder caused a reduction of l^* from $l^* = 5.2$ μm in the pure film to $l^* = 4.1$ μm in the TiO_2 doped polymer film. In Fig. (6) we plot the PFT of the random laser spectra for two polymer films, namely undoped and doped with TiO_2 particles, versus d/l^*. Our first observation is that, whereas the peaks in the PFTs of individual spectra appear to be uncorrelated, the averaging over 125 spots yields a remarkable periodicity in the peak positions. This is in accordance with the theoretical dependence that is implied in Eq. (5). The first harmonic near $d/l^* = 3$ differs by 20 percent from the data; this discrepancy is likely from the discreteness of the PFT. However, the discrepancy for the next five harmonics is maximum 6 percent. We thus conclude that the scaling is compelling.

In the same figure we also show a theoretical dependence, $\langle I(d)\rangle$, plotted using Eq. (5) that is superimposed on a smooth background obtained from the structureless component of the experimental PFTs in Fig. 6. The only fitting parameter in the theoretical $\langle I(d)\rangle$ is the dimensionless ratio d/l^*, which was set to be 2.9. It is seen that the theoretical $\langle I(d)\rangle$ curve exhibits the same saw-tooth structure as the experimental curves.

The fact that the peaks in the theoretical curve diminish much slower with d than in the experimental PFTs can be accounted for incomplete averaging, since the higher is the peak index, the higher is the statistical error.

5. Conclusions

Until now, two different regimes of random lasing have been addressed in the literature, namely, incoherent and coherent random lasing, respectively. They correspond to different parameters domains of scattering media with optical gain. Incoherent random lasing occurs when, in the absence of gain, the propagation of light is diffusive, i.e. $l^* \gg \lambda$. Coherent random lasing should take place below or near the threshold of the Anderson localization transition, when $l^* \lesssim \lambda$. In this paper we demonstrate, however, that in the presence of long-range inhomogeneities of the refraction index with characteristic scale $L \gg \lambda$ the coherent random lasing is also possible even when $l^* \gg \lambda$, so that *on average* the propagation of light is diffusive. This is because inhomogeneities may trap light within the scale $\sim L$ in a 'classical' fashion (due to total internal reflections). If $L \gg l^*$, which is the case for the polymer films that we have studied here, the areal density of resonators that are able to trap light decreases rapidly with L [roughly as $\exp(-L/l^*)$]. On the other hand, at the lasing threshold, resonators with the largest L lase first. These two opposite trends effectively 'fix' the value of L. As a result of L being approximately fixed, the positions of the emission lines are correlated. This correlation manifests itself in the shape of the average PFT of the emission spectra, which exhibits pronounced regular peaks.

Acknowledgements. We are grateful to D. Chinn at Sandia National Labatories who provided the microdisk samples. This work was supported by NSF Grant No. DMR 9732820, DOE Grant No. 96-ER45490, and the NSF Center for fibers at Clemson University.

References

[1] Y. Yamamoto, R.E. Slusher, Phys. Today 46 (1993) 66–73.
[2] C. Gmachl, F. Capasso, E.E. Narimanov, J.U. Nöckel, A.D. Stone, J. Faist, D.L. Sivco, A.Y. Cho, Science 280 (1998) 1556–1564.
[3] V.S. Letokhov, Zh. Eksp. Teor. Fiz. 53 (1967) 1442–1452, Sov. Phys. JETP 26 (1968) 835–840.
[4] A.Z. Genack, J.M. Drake, Nature (London) 368 (1994) 400–401.
[5] S. John, G. Pang, Phys. Rev. A 54 (1996) 3642–3652.
[6] D.S. Wiersma, A. Lagendijk, Phys. Rev. E 54 (1996) 4256–4265.
[7] M. Siddique, R.R. Alfano, G.A. Berger, M. Kempe, A.Z. Genack, Opt. Lett. 21 (1996) 450–452.
[8] G.A. Berger, M. Kempe, A.Z. Genack, Phys. Rev. E 56 (1997) 6118–6122.
[9] R.M. Balachandran, N.M. Lawandy, J.A. Moon, Opt. Lett. 22 (1997) 319–321.
[10] S. John, Phys. Rev. B 31 (1985) 304–309.
[11] S. John, Phys. Today 44 (5) (1991) 32–40.
[12] N. Garcia, A.Z. Genack, Phys. Rev. Lett. 66 (1991) 1850–1853.
[13] A.Z. Genack, N. Garcia, Phys. Rev. Lett. 66 (1991) 2064–2067.
[14] D.S. Wiersma, M.P. van Albada, B.A. van Tiggelen, A. Lagendijk, Phys. Rev. Lett. 75 (1995) 1739–1742.
[15] D.S. Wiersma, P. Bartolini, A. Lagendijk, R. Righini, Nature 390 (1997) 671–673.
[16] A.A. Chabanov, M. Stoytchev, A.Z. Genack, Nature 40 (2000) 850–853.
[17] P.A. Lee, R.A. Webb, in: B.A. Altshuler (Ed.), Mesoscopic Phenomena in Solids, North-Holland, Amsterdam, 1991.
[18] R. Berkovits, S. Feng, Phys. Rep. 238 (1994) 135–172.
[19] R. Pnini, B. Shapiro, Phys. Rev. B 39 (1989) 6986–6994.
[20] N.M. Lawandy, R.M. Balachandran, A.S.L. Gomes, E. Sauvain, Nature (London) 368 (1994) 436–438.
[21] D.S. Wiersma, M.P. van Albada, A. Lagendijk, Nature (London) 373 (1995) 203–204.
[22] W.L. Sha, C.H. Liu, R.R. Alfano, J. Opt. Soc. Am. B 19 (1994) 1922–1924.
[23] W. Zhang, N. Cue, K.M. Yoo, Opt. Lett. 20 (1995) 961–963.
[24] R.M. Balachandran, N.M. Lawandy, Opt. Lett. 20 (1995) 1271–1273.
[25] M.A. Noginov, H.J. Caufield, N.E. Noginova, P. Venkateswarlu, Opt. Commun. 118 (1995) 430–437.
[26] J. Martorell, R.M. Balachandran, N.M. Lawandy, Opt. Lett. 21 (1996) 239–241.
[27] R.M. Balachandran, D.P. Pacheo, N.M. Lawandy, Appl. Opt. 35 (1996) 640–643.
[28] W.L. Sha, C.H. Liu, F. Liu, R.R. Alfano, Opt. Lett. 21 (1996) 1277–1279.
[29] P.C. de Olivera, J.A. McGreevy, N.M. Lawandy, Opt. Lett. 22 (1997) 700–702.
[30] B.R. Prasad, H. Ramachandran, A.K. Sood, C.K. Subramanian, N. Kumar, Appl. Opt. 36 (1997) 7718–7724.
[31] G. Beckering, S.J. Zilker, D. Haarer, Opt. Lett. 22 (1997) 1427–1429.

[32] H.Z. Wang, F.L. Zhao, Y.J. He, X.G. Zheng, X.G. Huang, Opt. Lett. 23 (1998) 777–779.
[33] G. van Soest, M. Tomita, A. Lagendijk, Opt. Lett. 24 (1999) 306–308.
[34] G. Zacharakis, G. Heliotis, G. Filippidis, D. Anglos, T.G. Papazoglou, Appl. Opt. 38 (1999) 6087–6092.
[35] M. Shukri, R.L. Armstrong, Appl. Opt. 39 (2000) 4300–4305.
[36] V.M. Markushev, V.F. Zolin, M.Ch. Briskina, Sov. J. Quantum Electron. 16 (1986) 281–283.
[37] V.M. Ter-Gabrièlyan, N.È. Markushev, V.R. Belan, M.Ch. Briskina, V.F. Zolin, Sov. J. Quantum Electron. 21 (1991) 32–33.
[38] C. Gouedard, D. Husson, C. Sauteret, F. Auzel, A. Migus, J. Opt. Soc. Am. B 10 (1993) 2358–2363.
[39] F. Hide, B.J. Schwartz, M.A. Diaz-Garcia, A.J. Heeger, Chem. Phys. Lett. 256 (1996) 424–430.
[40] D.J. Denton, N. Tessler, M.A. Stevens, R.H. Friend, Adv. Mater. 9 (1997) 547–551.
[41] A.Yu. Zyuzin, Europhys. Lett. 26 (1994) 517–520.
[42] A.Yu. Zyuzin, Pis'ma Zh. Éksp. Teor. Fiz. 61 (1995) 961–963, JETP Lett. 61 (1995) 990–992.
[43] A.Yu. Zyuzin, Phys. Rev. E 51 (1995) 5274–5478.
[44] P. Pradhan, N. Kumar, Phys. Rev. B 50 (1994) 9644–9677.
[45] V. Freilikher, M. Pustilnik, I. Yurkevich, Phys. Rev. B 56 (1997) 5974–5977.
[46] C.W.J. Beenakker, J.C.J. Paasschens, P.W. Brouwer, Phys. Rev. Lett. 76 (1996) 1368–1371.
[47] J.C.J. Paasschens, T.Sh. Misirpashaev, C.W.J. Beenakker, Phys. Rev. B 54 (1996) 11887–11890.
[48] X. Jiang, C.M. Soukoulis, Phys. Rev. B 59 (1999) 6159–6166.
[49] X. Jiang, Q. Li, C.M. Soukoulis, Phys. Rev. B 59 (1999) R9007–R9010.
[50] X. Jiang, C.M. Soukoulis, Phys. Rev. Lett. 85 (2000) 70–73.
[51] X. Jiang, C.M. Soukoulis, cond-mat/0103042.
[52] H. Cao, Y.G. Zhao, S.T. Ho, E.W. Seelig, Q.H. Wang, R.P.H. Chang, Phys. Rev. Lett. 82 (1999) 2278–2281.
[53] H. Cao, J.Y. Xu, D.Z. Zhang, S.H. Chang, S.T. Ho, E.W. Seelig, X. Liu, R.P.H. Chang, Phys. Rev. Lett. 84 (2000) 5584–5587.
[54] S.V. Frolov, Z.V. Vardeny, K. Yoshino, A. Zakhidov, R.H. Baughman, Phys. Rev. B 59 (1999) R5284–R5487.
[55] S.V. Frolov, Z.V. Vardeny, K. Yoshino, A. Zakhidov, R.H. Baughman, Opt. Commun. 162 (1999) 241–246.
[56] G. Zacharakis, N.A. Papadogiannis, G. Filippidis, T.G. Papazoglou, Opt. Lett. 25 (2000) 923–925.
[57] H. Cao, private communication.
[58] R.C. Polson, A. Chipouline, Z.V. Vardeny, Adv. Mater. 13 (2001) 760–764.
[59] D. Wiersma, Nature 406 (2000) 132–133.
[60] S. Washburn, in: B.L. Altshuler, P.A. Lee, R.A. Webb (Eds.), Mesoscopic Phenomena in Solids, North-Holland, Amsterdam, 1991, p. 3.
[61] N.N. Barashkov, D.J. Guerrero, H.J. Olivos, J.P. Ferraris, Synth. Met. 75 (1995) 153–159.
[62] J. Huang, PhD thesis, University of Utah, 2000, unpublished.
[63] S.V. Frolov, Z.V. Vardeny, K. Yoshino, Phys. Rev. B 57 (1998) 9141–9147.
[64] M.E. Raikh, I.M. Ruzin, in: B.L. Altshuler, P.A. Lee, R.A. Webb (Eds.), Mesoscopic Phenomena in Solids, North-Holland, Amsterdam, 1991, p. 315.
[65] see, O.A. Starykh, Ph. Jacquod, E.E. Narimanov, A.D. Stone, Phys. Rev. E 62 (2000) 2078, and references therein.
[66] D. Hofstetter, R.L. Thornton, Opt. Lett. 22 (1997) 1831–1833.
[67] D. Hofstetter, R.L. Thornton, Appl. Phys. Lett. 72 (1998) 404–406.
[68] R.C. Polson, G. Levina, Z.V. Vardeny, Appl. Phys. Lett. 76 (2000) 3858–3860.
[69] Steel, Interferometry, 2nd ed., Cambridge University Press, Cambridge, 1982.